

X-ray diffraction from faulted zinc sulphide crystals undergoing phase transitions

M. T. SEBASTIAN*

Regional Research Laboratory, Trivandrum 695 019, India

Stacking faults in close-packed structures are not always distributed randomly. When they occur preferentially at certain layer spacings. In such cases the classical theories of X-ray scattering from randomly faulted close-packed structures break down and a probability distribution of faults has to be assumed to compute the diffraction effects. This probability distribution depends on the mechanism of the transformation in the material being studied. By recording the diffuse intensity distribution along reciprocal lattice rows perpendicular to the faults obtained from a partially transformed crystal it is possible to determine the nature of the faults involved and derive information about the mechanism of the transformation. The application of this method to investigate the mechanism of $2H \rightarrow 3C$ and $2H \rightarrow 6H$ transformations in ZnS , $Zn_xCd_{1-x}S$ and $Zn_xMn_{1-x}S$ is discussed. A three parameter model assuming different fault probabilities for deformation faulting at larger separations (α), at three-layer separations (β) and at two-layer separations (γ) has been developed, to compute theoretically the diffraction effects from the transforming crystals and explain the experimentally observed distribution of diffuse intensity in reciprocal space.

1. Introduction

Several materials with a close-packed structure, such as like ZnS , SiC and cobalt are known to undergo solid state structural transformations from one ordered structure to another through the insertion of stacking faults. The nature of the stacking faults involved in the transformation and their distribution can be determined by arresting the transformation at an intermediate stage and studying the disordered partially transformed crystal by X-ray diffraction techniques.

2. Stacking faults in close-packed structures

In a close-packed structure the stacking rule is occasionally broken resulting in the occurrence of a stacking fault. Such a stacking fault does not alter the number of nearest neighbours and often even their separation, causing very little change in the binding energy of the structure. In such cases the stacking faults may occur in sufficient concentration to produce visible diffraction effects on X-ray diffraction photographs. The different kinds of stacking faults that can occur are:

(i) Growth faults: if a stacking fault results by the incorrect addition of a single layer during the layer by layer growth of a crystal and the subsequent layers follow the stacking rule it is known as a growth fault. The growth fault configurations in the hcp (2H) and fcc (3C) structures are depicted as:

Growth fault in a 2H structure: ABABCBCB . . .

Growth (or twin) fault in a 3C structure:

ABCABCBCBA . . .

The position of the fault plane is indicated by underlining.

(ii) Deformation faults: if two parts of the crystal slip past each other along the basal plane through a partial slip vector $\pm S_i$ where S_i denotes $S_1 = (a/3)[1\bar{1}00]$, $S_2 = (a/3)[01\bar{1}0]$ and $S_3 = (a/3)[\bar{1}010]$, then it produces a deformation fault. Such a fault configuration is depicted below for the 2H and 3C structures.

Deformation fault in a 2H structure:

ABAB|CACACA . . .

Deformation fault in a 3C structure:

ABCABC|BCABCA . . .

The position of the fault plane is indicated by the vertical line.

(iii) Layer displacement fault: a layer displacement fault can nucleate in the original structure by the aggregation of vacancies at high temperatures in a small region of a close-packed layer and then expand by the diffusion of neighbouring atoms in accordance with the mechanism suggested by Pandey *et al.* [1]. Such a fault configuration displaces only one or two layers in the structure leaving all the other layers unaffected, as depicted below:

Perfect 2H structure : ABAB|A|BAB . . .

Faulted 2H structure: ABAB|C|BAB . . .

Perfect 3C structure : ABCAB|CA|BC . . .

Faulted 3C structure: ABCAB|AC|BC . . .

where the displaced layers are indicated by the rectangles.

* Present address: Laboratoire de Mineralogie-Cristallographie, Université de Pierre et Marie Curie, 75252 Paris, Cedex 05, France.

(iv) Extrinsic faults: such faults occur by the insertion or removal of a whole layer in a close-packed structure. They are faults of much higher energy and therefore uncommon.

Extrinsic fault in a 2H structure: ABABCAB . . .

Extrinsic fault in a 3C structure: ABCABABC . . .

or

ABCABC|BCABCA

The extra layer is indicated by underlining and the missing layer by a vertical bar.

3. The distribution of stacking faults

Close-packed structures of different inorganic compounds generally exist in certain small period basic structures which occur more frequently. The basic structures for ZnS are 2H and 3C whereas for SiC they are 6H, 15R and 4H. Similarly the basic structures for CdI₂ are 2H and 4H. Stacking faults in these materials can occur either randomly, non-randomly or periodically. Accordingly three different situations arise.

(i) When the faults are distributed randomly, the probability of faulting can be assumed to be the same on every layer and the classical theories of X-ray scattering from one-dimensionally disordered structures, summarized by Warren [2] and Sebastian and Krishna [3] can be applied. Such situations arise when the stacking faults occur as accidents and their concentration is low.

(ii) When the faults are distributed non-randomly, the probability of faulting cannot be assumed to be the same on every layer and the classical theories of X-ray scattering from one-dimensionally disordered structures break down. One has then to introduce probability distribution for the faults and compute the diffraction effects. Such a situation arises when the faults occur in the course of a phase transformation and therefore have preferred sites for their occurrence. The probability distribution of the faults is related to the mechanism of the transformation and thus provides information about it. This is discussed in greater detail in the next section.

(iii) When the faults occur periodically they give rise to a long-period polytype structure. The periodic occurrence may be either due to a screw dislocation mechanism [4] or in metallic systems due to the lowering of the energy of the conduction electrons. In the latter case the long-period structures are called superlattices and usually occur at specific compositions in an alloy. In this case one obtains a completely new structure with well-defined sharp X-ray reflections, corresponding to the well-defined reciprocal lattice of the polytype or superlattice structure. The diffraction effects from such ordered long-period structures have been discussed in detail by Verma and Krishna [4].

4. X-ray diffraction from a randomly faulted close-packed structure

The presence of random stacking faults in a crystal destroys the periodicity parallel to the stacking axis which renders one of the three Laue conditions invalid.

This gives rise to diffuse streaks depending on the amount of disorder present in the crystal. The first theoretical treatments of X-ray scattering from such disordered structures were reported by Wilson [5] and Hendricks and Teller [6]. Since then several workers [2, 7–14] have developed the theory of X-ray diffraction from crystals containing a random distribution of stacking faults. The theory predicts changes in integrated intensity, peak positions and half widths of reflections for which $H - K \neq 0 \pmod{3}$. By measuring these experimentally, it is possible to evaluate the degree of faulting in the crystals. A considerable amount of the experimental work has been done using powder samples to determine the nature of stacking faults and the fault concentration by studying line widths and peak shifts [23]. The information so obtained gives values that are averaged over all the grains in the powder sample. Such a method is obviously unsuitable for the study of polytypic materials where different grains could possess different crystal structures. Single crystal studies provide much more reliable information about the disorder in individual crystals, but very few such studies have been reported in the literature.

Recently, we have made a systematic analysis of the nature of stacking faults in 2H and 3C ZnS crystals [15–17]. As-grown and annealed disordered 2H crystals are found to contain a random distribution of deformation faults whereas in disordered 3C crystals a random distribution of twin (growth) faults are present.

5. Diffraction effects from crystals of ZnS, Zn_xCd_{1-x}S and Zn_xMn_{1-x}S undergoing phase transformation

The 2H (wurtzite) modification of ZnS is metastable at temperatures below 1020°C and undergoes solid state transformation to the 3C phase [15–20]. Many of the crystals are found [15] to show weak X-ray reflections near the 6H positions. The 2H → 3C transformation in ZnS crystals commences with the insertion of deformation faults [15, 19]. A non-random insertion of deformation faults at two-layer separations can effect the 2H → 3C transformation as depicted below:

Initial structure (2H) : AB|ABABAB
 CA|CACA
 BC|BC
 AB

Resulting structure (3C) : ABCABCAB

It is found [21–24] that solid solutions of ZnS with a little CdS or MnS undergo a 2H–6H transformation on annealing. Such a transformation can be effected by a non-random insertion of deformation faults at three-layer separations as shown below:

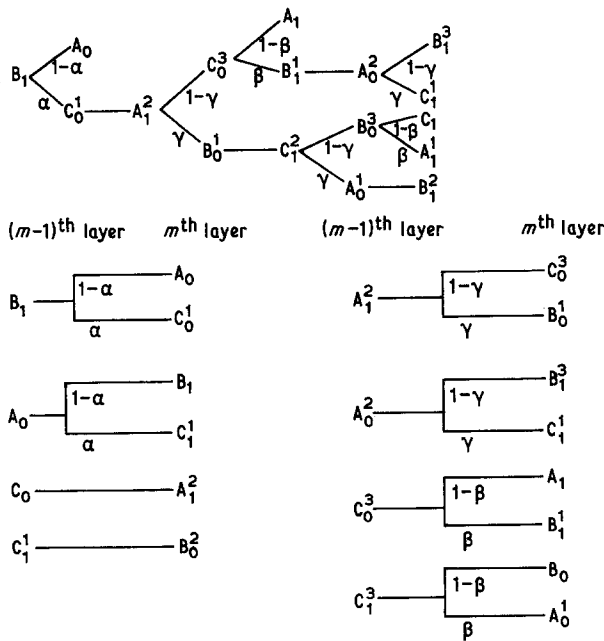
Initial structure (2H) : AB|ABA BABAB
 CAC|ACACA
 BAB|AB
 CA

Resulting structure (6H) : ABCACBABCA

X-ray diffractograms recorded from partially transformed crystals reveal a marked enhancement of intensity at the positions corresponding to 6H reflections during the 2H → 3C transformation and conversely an intensity enhancement at the 3C positions during the 2H → 6H transformation. Figs 1 and 2 show the single crystal diffractometer records of intensity against L in reciprocal space for 2H ZnS crystals at different stages of transformation to the 3C structure, and Fig. 3 shows that of a 2H $\text{Zn}_{0.94}\text{Cd}_{0.06}\text{S}$ crystal partially transformed to a 6H structure. It is evident from the figures that the faults have a higher probability of nucleating at two- and three-layer separations. In order to explain the observed intensity distribution we have therefore developed a general three-parameter model for the computation of diffraction effects. The model makes the following assumptions:

- (i) the crystal is infinite in size and free of distortions;
- (ii) the scattering power for all the layers is the same;
- (iii) there is no change in the layer spacings at the faults;
- (iv) the faults extend right across the crystal;
- (v) the effect of absorption, thermal diffuse scattering and scattering from point defects is negligible;
- (vi) the probability for faults to nucleate at random at large separations is α which is different from the probability β for the faults to occur at three-layer separations and the probability γ for them to occur at two-layer separations. The probability for faults to occur on successive layers is negligible.

Employing the notations used earlier [1, 24, 25] the fault probability trees for such a three-parameter model of the transformation can be written as follows:



Following Sebastian and Krishna [24, 25] we obtain the following difference equations from the probability trees.

$$J_{(m,0)} = (1 - \alpha)J_{(m-1,1)}\omega_2 + (1 - \beta)J_{(m-1,3)}\omega_2 \quad (1)$$

$$J_{(m,1)} = (1 - \alpha)J_{(m-1,0)}\omega_1 + (1 - \beta)J_{(m-1,0^3)}\omega_1 \quad (2)$$

$$J_{(m,0^1)} = \alpha J_{(m-1,1)}\omega_1 + \beta J_{(m-1,1^3)}\omega_1 + \gamma J_{(m-1,1^2)}\omega_1 \quad (3)$$

$$J_{(m,1^1)} = \alpha J_{(m-1,0)}\omega_2 + \beta J_{(m-1,0^3)}\omega_2 + \gamma J_{(m-1,0^2)}\omega_2 \quad (4)$$

$$J_{(m,0^2)} = J_{(m-1,1^1)}\omega_2 \quad (5)$$

$$J_{(m,1^2)} = J_{(m-1,0^1)}\omega_1 \quad (6)$$

$$J_{(m,0^3)} = (1 - \gamma)J_{(m-1,1^2)}\omega_2 \quad (7)$$

$$J_{(m,1^3)} = (1 - \gamma)J_{(m-1,0^2)}\omega_1 \quad (8)$$

On trying a solution of the form $J_{(m,j)} = C_j^m, q^m \geq 0$ and eliminating the various C_s we get the following characteristic equation:

$$\begin{aligned} q^8 + [\gamma - (1 - \alpha)^2]q^6 + [\alpha(1 - \beta)(1 - \gamma) \\ + \gamma^2 - \gamma(1 - \alpha)^2]q^4 + [\beta^2(2\gamma - 1) \\ + 2\alpha\gamma(1 - \beta) - \gamma^2 - \gamma^2(\alpha - \beta)^2]q^2 \\ + (1 - \gamma)^2(\alpha - \beta)^2 = 0 \end{aligned} \quad (9)$$

Following Holloway [26] and Sebastian and Krishna [21, 25] the expression for the diffracted intensity can be written as

$$I = f^2 C \left[\left(\frac{1}{2} + \frac{P}{Q} \right) + \text{complex conjugate} \right] \quad (10)$$

where

$$\begin{aligned} P &= T_1 e^{7i\pi L} + T_2 e^{6i\pi L} + (T_3 + a_6 T_1) e^{5i\pi L} \\ &+ (T_4 + a_6 T_2) e^{4i\pi L} + (T_5 + a_6 T_3 + a_4 T_1) e^{3i\pi L} \\ &+ (T_6 + a_6 T_4 + a_4 T_2) e^{2i\pi L} \\ &+ (T_7 + a_6 T_5 + a_4 T_3 + a_2 T_1) e^{i\pi L} - a_0 \\ Q &= a_0 + a_2 e^{2i\pi L} + a_4 e^{4i\pi L} + a_6 e^{6i\pi L} + e^{8i\pi L} \\ f^2 &= f_{Zn}^2 + f_S^2 + 2f_{Zn}f_S \cos \frac{3\pi L}{4} \end{aligned}$$

C is a scale factor,

$$\begin{aligned} a_6 &= \gamma - (1 - \alpha)^2 \\ a_4 &= \alpha(1 - \beta)(1 - \gamma) + \gamma^2 - \gamma(1 - \alpha)^2 \\ a_2 &= \beta^2(2\gamma - 1) + 2\alpha\gamma(1 - \beta) - \gamma^2[1 + (\alpha - \beta)^2] \\ a_0 &= (1 - \gamma)^2(\alpha - \beta)^2 \\ T_1 &= -\frac{1}{2} \\ T_2 &= (1 - \beta - \gamma + \beta\gamma - \alpha\gamma)/x \\ T_3 &= (-1 + \beta + \gamma - \beta\gamma + 4\alpha\gamma)/2x \\ T_4 &= (1 - 3\alpha - \beta - \gamma + 3\alpha\beta + 2\alpha\gamma + \beta\gamma - 3\alpha\beta\gamma)/x \\ T_5 &= (-1 + 3\alpha + \beta + \gamma - \beta\gamma + \alpha\gamma + 3\alpha^2 - 6\alpha\beta \\ &\quad - 6\alpha\gamma^2 + 6\alpha\beta\gamma - 3\alpha^2\beta - 3\alpha^2\gamma + 3\alpha^2\beta\gamma)/2x \\ T_6 &= (1 - 6\alpha - \beta - \gamma + 9\alpha\beta + 5\alpha\gamma + \beta\gamma + 6\alpha^2 \\ &\quad - 3\alpha^3 - 12\alpha\beta\gamma - 6\alpha^2\beta - 6\alpha^2\gamma + 3\alpha\gamma^2 \\ &\quad + 3\alpha^3\gamma + 6\alpha^2\beta\gamma + 3\alpha^3\beta + 3\alpha\beta\gamma^2 - 3\alpha^3\beta\gamma)/x \end{aligned}$$

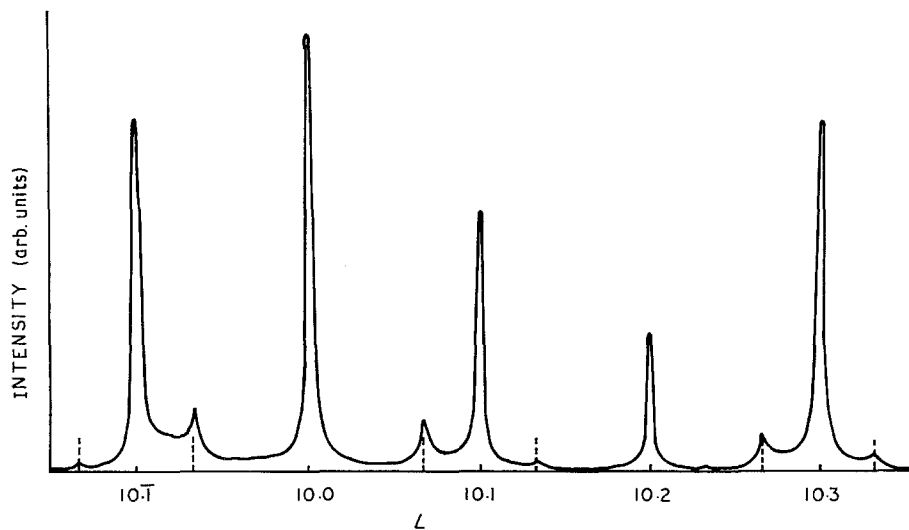


Figure 1 Single crystal diffractometer plot of intensity against L along the $10.L$ reciprocal lattice row for a disordered 2H crystal obtained by annealing a perfect 2H ZnS crystal.

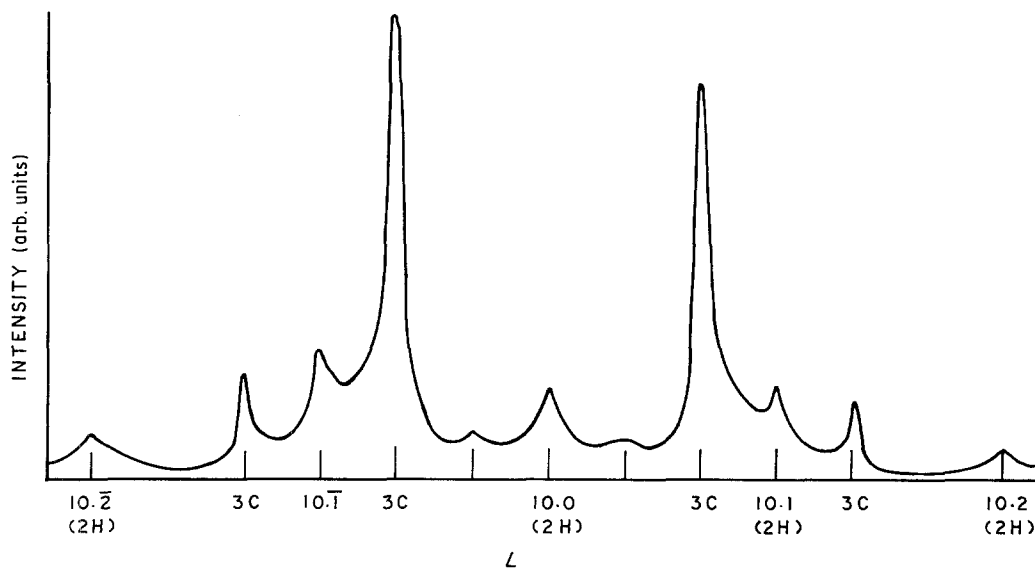


Figure 2 Single crystal diffractometer plot of intensity against L along the $10.L$ reciprocal lattice row for a nearly transformed disordered twinned 3C ZnS crystal with intensity enhancement near the 6H positions. The vertical lines indicate the 6H positions.

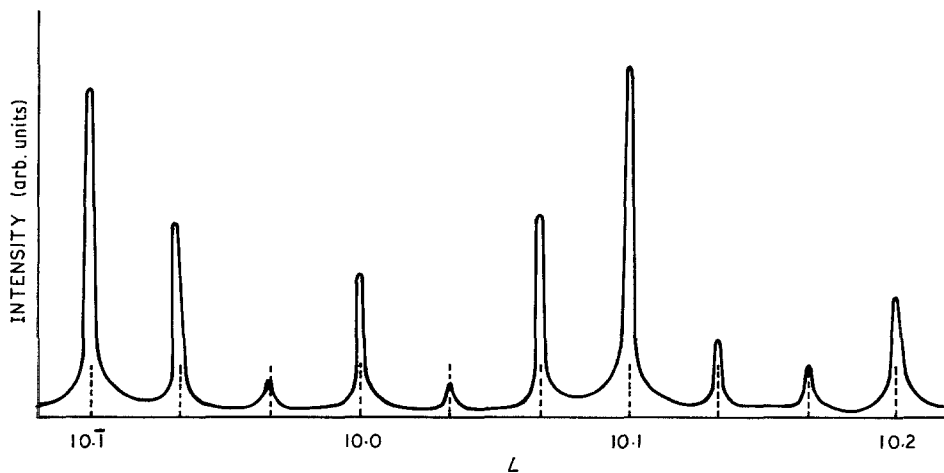


Figure 3 Single crystal diffractometer plot of intensity against L along the $10.L$ reciprocal lattice row for a 2H $Zn_{0.94}Cd_{0.06}S$ crystal partially transformed to the 6H obtained by annealing a 2H crystal at $800^{\circ}C$ for 1 h. The vertical lines indicate the 6H positions.

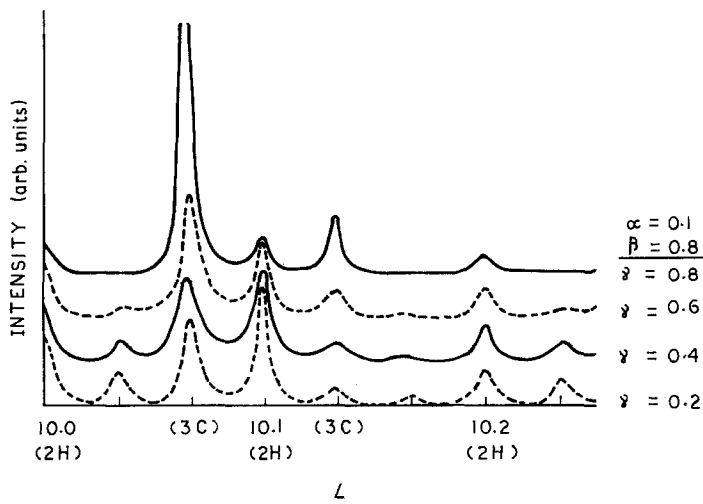


Figure 4 Calculated variation of the diffracted intensity along the $10.L$ reciprocal lattice row for a 2H crystal undergoing transformation by the three-parameter model for $\alpha = 0.1$; $\beta = 0.8$ and $\gamma = 0.2, 0.4, 0.6$ and 0.8 . The calculated profiles are shifted vertically for clarity. The vertical lines indicate the 6H positions.

$$T_7 = (-1 + 6\alpha + \beta + \gamma - 3\alpha^2 - \beta\gamma - 12\alpha\beta - 2\alpha\gamma + 18\alpha\beta\gamma + 3\alpha\beta^2 - 9\alpha^2\gamma + 3\alpha^2\beta - 9\alpha\gamma^2 + 6\alpha\beta\gamma^2 + 3\alpha\gamma^3 + 3\alpha^4 + 12\alpha^2\gamma^2 + 9\alpha^2\beta\gamma - 6\alpha\beta^2\gamma - 3\alpha^4\gamma - 12\alpha^2\beta\gamma^2 - 3\alpha^4\beta - 3\alpha^3\beta^2\gamma + 3\alpha\beta^2\gamma^2 + 3\alpha^2\beta^2\gamma)/2x$$

$$x = 1 + 3\alpha - \beta - \gamma + \beta\gamma - \alpha\gamma.$$

Using Equation 10 the diffracted intensity along the $10.L$ reciprocal lattice row was computed for values of L varying in steps of 0.01 using various values of α , β and γ . Fig. 4 shows the calculated distribution along the $10.L$ reciprocal lattice row as computed for $\alpha = 0.1$, $\beta = 0.8$ and γ varying from 0.2 to 0.8. Fig. 5 shows the calculated intensity distribution as obtained for $\alpha = 0.1$, $\gamma = 0.4$ and β varying from 0.2 to 0.9.

6. Comparison with experiment

The above theoretical model for the calculation of diffracted intensity enables us to calculate the intensity distribution:

- (i) for the 2H \rightarrow 3C transformation by preferential faulting at two-layer separations if we put $\beta = \alpha$;
- (ii) for the 2H \rightarrow 6H transformation by preferential faulting at three-layer separations if we put $\gamma = 0$, and

(iii) for the general case, of transformation where neither β nor γ is zero.

In comparing the calculated profiles with those observed experimentally, two possibilities need to be considered.

(a) The 2H \rightarrow 3C and 2H \rightarrow 6H transformations may occur separately in different regions of the crystal. In this case the resulting intensity profile would be an addition of the intensity profiles for the 2H \rightarrow 3C and 2H \rightarrow 6H transformations in a suitable proportion.

(b) The transformation occurs homogeneously in all regions of the crystal with a preferential fault probability β at three-layer separations and γ at two-layer separations. In this case the resultant intensity would be that given by the three-parameter model and it should be possible to determine the values of α , β and γ for each recorded profile.

Analysis of the experimentally observed diffraction effects obtained by us favour possibility (a) as against possibility (b). Figs 6 and 7 show the calculated variation of the diffracted intensity for a mixture of the 2H \rightarrow 6H and 2H \rightarrow 3C transformations with $\alpha = 0.04$ and $\alpha = 0.3$, respectively. A comparison of the experimentally recorded intensity profiles in different stages of the 2H-3C and 2H-6H transformations with those computed theoretically using the three-parameter model with different values of α , β and γ

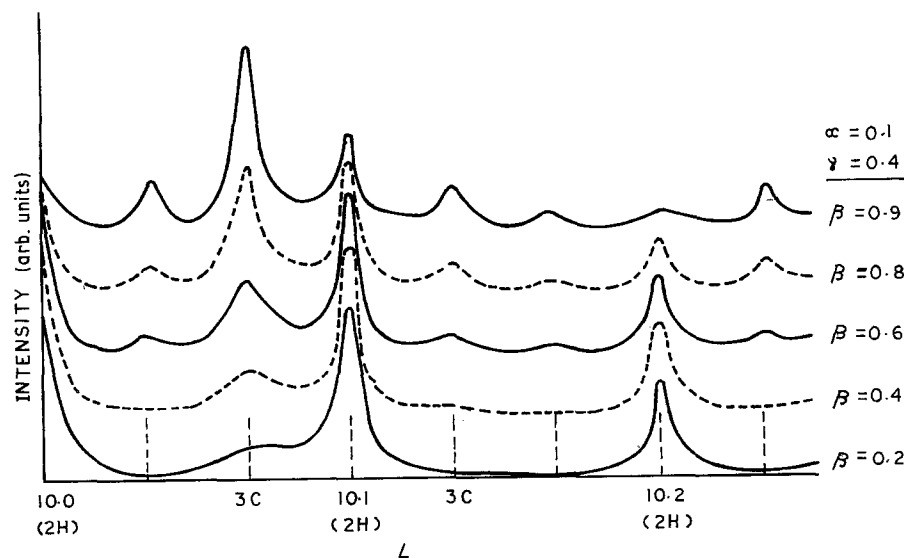


Figure 5 Calculated variation of the diffracted intensity along the $10.L$ reciprocal lattice row for a 2H crystal undergoing transformation by the three-parameter model for $\alpha = 0.1$, $\gamma = 0.4$ and $\beta = 0.2, 0.4, 0.6, 0.8$ and 0.9 . The calculated profiles are shifted vertically for clarity.

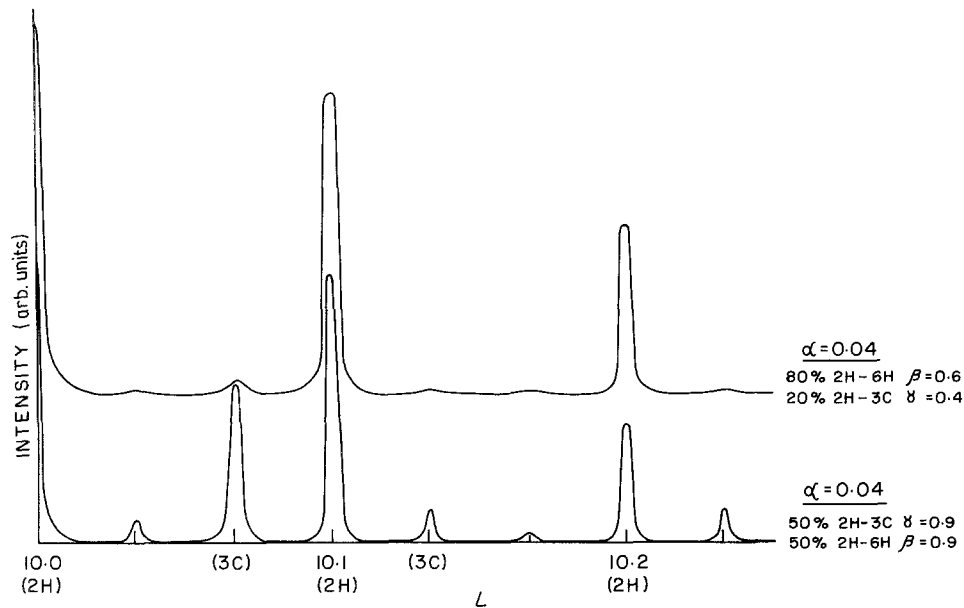


Figure 6 Calculated variation of the diffracted intensity for a mixture of 2H \rightarrow 6H and 2H \rightarrow 3C transformation for $\alpha = 0.04$. (a) 50% 2H \rightarrow 3C with $\gamma = 0.9$ and 50% 2H \rightarrow 6H with $\beta = 0.9$. (b) 80% 2H \rightarrow 6H with $\beta = 0.6$ and 20% 2H \rightarrow 3C with $\gamma = 0.4$.

shows that the model is not applicable as such to these crystals. During the 2H–3C transformation the theory predicts the shift of the intensity of those 6H reflections which do not coincide with the cubic peaks ($L = \pm\frac{1}{3}, \pm\frac{2}{3}$) towards the nearby 3C positions. Experimentally recorded profiles do not show any shift of these reflections. The peak broadening for these crystals is also not in good agreement with the predicted values. The experimental profiles (Figs 1 to 3) are found to be in reasonable agreement with those computed theoretically for a suitable mixture of the 2H \rightarrow 3C and 2H \rightarrow 6H transformations. As the transformation behaviour is composition dependent this may be due to slight variations of the composition (impurity content) in the different regions of the same single crystal. It is known that the addition of small quantities of CdS or MnS to ZnS stabilizes the 6H phase; consequently, a different proportion of transformation to the 3C and 6H structure in different

regions of the same single crystal is possible in the solid solution phases though it is somewhat surprising in ZnS itself. Singer [27] also observed the presence of such independently diffracting domains in ZnS crystals; the independent scattering from such domains being additive. The enhancement of the diffracted intensity near the 6H positions was also observed by Fleet [28] in mineral sphalerite (3C) ZnS crystals which were believed to have formed from the wurtzite phase. Steinberger [29] and Mardix [30] have observed the presence of a large number of regions varying in width and each representing a particular polytype structure. It should be noted that the periodic slip mechanism proposed for the 2H–3C transformation in ZnS proposed by Mardix and Steinberger [31] and Daniels [32] can operate only in those crystals which have an axial screw dislocation. A small value of α and a large value of β represents this situation at an intermediate state.

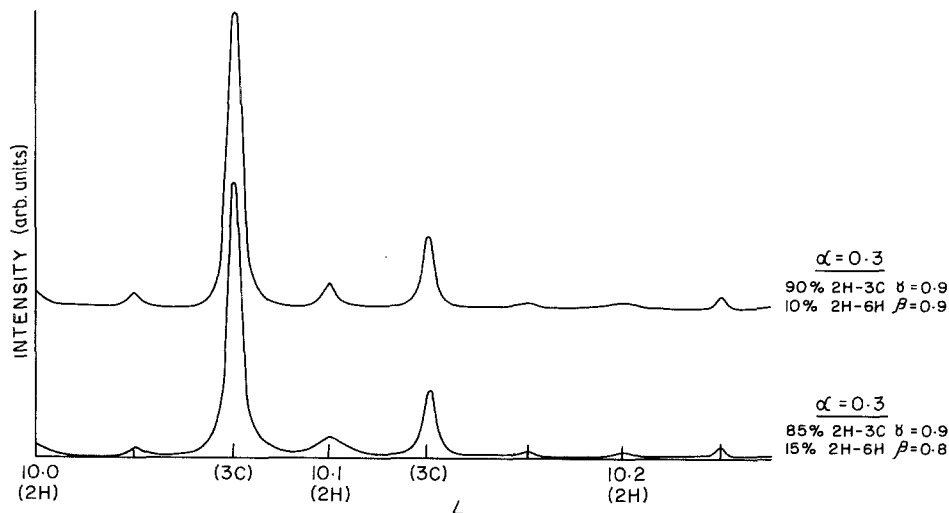


Figure 7 Calculated variation of the diffracted intensity for a mixture of 2H \rightarrow 6H and 2H \rightarrow 3C transformation for $\alpha = 0.3$. (a) 85% 2H \rightarrow 3C with $\gamma = 0.9$ and 15% 2H \rightarrow 6H with $\beta = 0.8$. (b) 90% 2H \rightarrow 3C with $\gamma = 0.9$ and 10% 2H \rightarrow 6H with $\beta = 0.9$.

7. Conclusions

The 2H → 3C transformation in ZnS occurs through the non-random nucleation of deformation faults occurring preferentially at two-layer separations. The addition of a little CdS or MnS, to form solid solutions of the type $Zn_xCd_{1-x}S$ and $Zn_xMn_{1-x}S$ ($x \geq 0.9$) causes the phase transformation to occur through a 6H phase. The 2H → 6H transformation occurs by the non-random nucleation of deformation faults occurring preferentially at three-layer separations. Several crystals of the solid solutions show a mixture of both transformations on their X-ray diffraction photographs in different proportions. Comparison of the observed diffraction effects with those computed theoretically using a three-parameter probability distribution of faults, confirms that the 2H → 3C and 2H → 6H transformations take place simultaneously in different regions of the same single crystal.

Acknowledgement

The author thanks Professor P. Krishna (B.H.U.) for many helpful discussions.

References

1. D. PANDEY, S. LELE and P. KRISHNA, *Proc. Roy. Soc. A* **369** (1980) 435.
2. B. E. WARREN, "X-ray Diffraction" (Addison-Wesley, New York, 1969).
3. M. T. SEBASTIAN and P. KRISHNA, "Progress in Crystal Growth and Characterization" **14** (1987) 103.
4. A. R. VERMA and P. KRISHNA, "Polymorphism and Polytypism in Crystals" (Wiley, New York, 1966).
5. A. J. C. WILSON, *Proc. Roy. Soc. A* **180** (1942) 277.
6. S. B. HENDRICKS and E. TELLER, *J. Chem. Phys.* **10** (1942) 147.
7. H. JAGODZINSKI, *Acta Crystallogr.* **2** (1949) 208.
8. *Idem, ibid.* **2** (1949) 298.
9. M. S. PATERSON, *J. Appl. Phys.* **23** (1952) 805.
10. R. GEVERS, *Acta Crystallogr.* **5** (1952) 518.
11. *Idem, ibid.* **7** (1954) 337.
12. J. W. CHRISTIAN, *ibid.* **7** (1954) 415.
13. J. KAKINOKI, *ibid.* **23** (1963) 1973.
14. R. BERLINER and S. A. WERNER, *Phys. Rev. B* **34** (1986) 3586.
15. M. T. SEBASTIAN, D. PANDEY and P. KRISHNA, *Phys. Status Solidi (a)* **71** (1982) 633.
16. M. T. SEBASTIAN and P. KRISHNA, *Phil. Mag.* **49** (1984) 809.
17. M. T. SEBASTIAN and P. KRISHNA, *Pramana* **23** (1984) 395.
18. H. MÜLLER, *Neues. Jb. Miner Abb* **84** (1952) 43.
19. W. L. ROTH, "Faulting in ZnS", General Electric Research Lab. Report No. 60-RI-2563m, Schenectady, New York (1960).
20. A. ADDAMIANO and M. AVEN, *J. Appl. Phys.* **31** (1960) 36.
21. M. T. SEBASTIAN and P. KRISHNA, *Phys. Status Solidi (a)* **79** (1983) 271.
22. *Idem, Solid State Commun.* **49** (1983) 879.
23. *Idem, J. Crystal Growth* **66** (1984) 586.
24. *Idem, Bull. Mater. Sci.* **6** (1984) 369.
25. *Idem, Phys. Status Solidi a* **84** (1984) 401.
26. H. HOLLOWAY, *J. Appl. Phys.* **40** (1969) 4313.
27. J. SINGER, *Acta Crystallogr.* **16** (1963) 601.
28. M. E. FLEET, *Amer. Mineral.* **62** (1977) 540.
29. I. T. STEINBERGER, "Crystal Growth and Characterisation of Polytype Structures", edited by P. Krishna (Pergamon, Oxford, 1983).
30. S. MARDIX, *J. Appl. Crystallogr.* **17** (1984) 328.
31. S. MARDIX and I. T. STEINBERGER, *Isr. J. Chem.* **3** (1966/67) 243.
32. B. K. DANIELS, *Phil. Mag.* **14** (1966) 487.

Received 30 March
and accepted 16 June 1987